CRISPR gene-drive systems based on Cas9 nickases promote super-Mendelian inheritance in *Drosophila*

Víctor López Del Amo[1,*], Sara Sanz Juste[1], Valentino M. Gantz[1,*]

[1] Section of Cell and Developmental Biology, University of California San Diego, La Jolla, CA 92093, USA

*Correspondence: vlopezdelamo@ucsd.edu (V.L.D.A) vgantz@ucsd.edu (V.M.G);

ABSTRACT

CRISPR-based gene drive systems can be used to modify entire wild populations due to their ability to bias their own inheritance towards super-Mendelian rates (>100%). Current gene drives contain a Cas9 and a gRNA gene inserted at the location targeted by the gRNA. These gene products are able to cut the opposing wildtype allele, and lead to its replacement with a copy of the gene drive through the homology-directed DNA repair pathway. When this allelic conversion occurs in the germline it leads to the preferential inheritance of the engineered allele — a property that has been proposed to disseminate engineered traits for managing disease-transmitting mosquito populations. Here, we report a novel gene-drive strategy relying on Cas9 nickases which operates by generating staggered paired-nicks in the DNA to promote propagation of the gene drive allele. We show that only when 5' overhangs are generated, the system efficiently leads to allelic conversion. Further, the nickase gene-drive arrangement produces large stereotyped deletions, providing potential advantages for targeting essential genes. Indeed, the nickase-gene-drive design should expand the options available for gene drive designs aimed at applications in mosquitoes and beyond.

Keywords: CRISPR, gene drives, nickase, HDR, *Drosophila*

INTRODUCTION

Mendel's first law of gene segregation determines that a specific allele has a 50% probability of being passed to the next generation in sexually reproducing organisms. CRISPR gene drive systems instead can bypass this inheritance limit and have emerged as a promising tool for disseminating engineered traits for population engineering. This proof-of-concept system first implemented in flies (Gantz and Bier, 2015), has been rapidly applied to different mosquitoes such as *Anopheles* or *Aedes* aiming to fight vector-borne diseases by modifying or suppressing insect populations under laboratory conditions (Adolfi et al., 2020; Gantz et al., 2015; Hammond et al., 2016; Kyrou et al., 2018; Li et al., 2020; Simoni et al., 2020).

CRISPR-based gene drives consist of a three-component transgene: (i) Cas9, a DNA nuclease capable of producing DNA double-strand breaks, (ii) a guide RNA (gRNA) that directs Cas9 to cleave the DNA at a predetermined site, and (iii) two homology arms flanking the Cas9/gRNA components; these homology arms match perfectly both sides of the cut site to promote homology-directed repair (HDR). When a gene drive individual mates a wildtype, these engineered gene drives utilize their encoded Cas9 to cut the wildtype allele in the germline, which is then replaced by HDR using the intact gene-drive chromosome as a template for repair. As this allelic conversion process occurs in the germline, heterozygous cells are converted to homozygosity. Given that the gene drive is now present on both alleles, this process produces a super-Mendelian inheritance of the engineered cassette (>50%), allowing gene drives to spread through a population while bringing along new traits.

While current gene-drive methods employ a Cas9 which introduces DNA double-strand breaks (Adolfi et al., 2020; Bier, 2021; Gantz et al., 2015; Hammond et al., 2016; Kyrou et al., 2018; Li et al., 2020; Simoni et al., 2020), mutant versions of Cas9 that generate only nicks instead of double-strand breaks should also be amenable to be used in a gene drive setting. The regular Cas9 is able to introduce DNA double-strand breaks as it contains two endonuclease domains (HNH and RuvC-like domains), each cleaving one of the strands of a DNA double-helix. However, mutations in critical residues within either of the nuclease domains provide with two nickase versions of Cas9: i) the nCas9-D10A (nD10A) containing the RuvC domain inactivated cuts the target strand where the gRNA is bound, and ii) the nCas9-H840A (nH840A), where the HNH activity is blocked; this version cleaves the non-target strand (Jinek et al., 2012).

The nD10A has been used to generate paired DNA-nicks and was shown to efficiently disrupt genes in *Drosophila* and cell culture (Gopalappa et al., 2018; Port et al., 2014). Additionally, DNA paired-nicks have shown to promote HDR *in vitro*, yet the nicks induced by nD10A were more efficient at promoting HDR when compared to the nH840A, where HDR rates were almost undetectable (Bothmer et al., 2017; Hyodo et al., 2020; Mali et al., 2013; Wang et al., 2021, 2018). Further, the nD10A can also boost specificity while reducing off-target effects since they require two gRNAs targeting each complementary DNA strand to either disrupt a gene function or trigger HDR. The combination of the same pair of gRNAs with the regular Cas9 generated undesired off-targets

effects at an unspecific genomic region, instead, the nD10A combined with the same gRNAs couple did not produce detectable off-target events (Ran et al., 2013).

While nickase Cas9 (nCas9) versions have been successfully utilized *in vitro*, to the best of our knowledge, none paired-gRNAs' nickase-based approaches have demonstrated efficient HDR in the germline of a living organism. We wondered whether a gene drive method based on nickase Cas9 could bring potential advantages for population engineering. For example, DNA nicks are involved in important biological processes such as DNA replication and are typically repaired efficiently (Caldecott, 2008; Chafin et al., 2000; Reyes et al., 2021; Wang and Hays, 2007). Therefore, if paired-nicks do not occur simultaneously, single nicks should restore the original wildtype sequence, reducing the formation of mutations or resistant alleles at the target site to allow further gene drive conversion. Additionally, DNA nicks follow distinct DNA repair pathways compared to DNA-double strand breaks introduced by traditional gene drives(Vriend and Krawczyk, 2017), and it is possible that the intrinsically offset distance between paired-nicks in a gene-drive setting promotes the formation of specific mutations that could be used to improve gene-drive efficiency in certain situations.

Thus, we hypothesize that simultaneous paired-nicks targeting two adjacent DNA regions should generate a staggered double-strand break, and subsequent DNA repair by HDR to promote super-Mendelian inheritance of an engineered gene-drive construct. Therefore, the scope of this work is to obtain a proof-of-concept nickase-based gene-drive system promoting super-Mendelian inheritance using *Drosophila melanogaster*. Indeed, we were able to develop and test a nickase gene-drive system and demonstrate that both nD10A and nH840A can promote efficient HDR in the germline. Interestingly, our results show that super-Mendelian inheritance rates can be achieved only when the gene-drive design generates 5’ overhangs. Furthermore, we show that the nH840A produces larger deletions compared to the nD10A when the allelic conversion fails, a property that could be employed to ensure gene-drive spread when targeting essential genes and simultaneously providing a rescue for the disrupted gene as part of the driven cassette.

RESULTS

A nickase gene drive system induces 5' or 3' overhangs depending on the gRNAs design and nickase version employed

To design a nickase-based gene drive system, we chose to use a gRNA-only split-drive system, also known as Copycat that consists of two separate components. First, a transgenic fly is carrying a static Cas9 transgene, which is inherited in a Mendelian fashion. Second, an engineered animal carrying a CopyCat cassette formed by a gRNA gene flanked by two homology arms (Gantz and Bier, 2016). Once the two components are placed together by genetic cross, traditional CopyCat gene drives (CC-GD) rely on DNA double-strand breaks produced by a single gRNA, which targets the same sequence on the wildtype allele where it is inserted to propagate the synthetic cassette by HDR (Champer et al., 2019; Gantz and Bier, 2016; López Del Amo et al., 2020a; Xu et al., 2017) (**Fig.1a**). In contrast, a nickase-based gene drive system requires two gRNAs since this modified Cas9 introduces DNA nicks instead of DNA double-strand breaks. In this case, the gRNA couple will produce two independent cleavage events on each of the DNA complementary strands to allow gene drive propagation by HDR, emulating the traditional gene-drives (**Fig.1b**).

To build a gene drive system based on a nCas9, we generated two transgenic lines containing a DsRed marker and carrying either the nD10A or nH840A versions, which cut the target strand (bound to the gRNA) or the non-target strand, respectively. Additionally, we employed a previously-validated regular Cas9 line, which introduces DNA double-strand breaks(López Del Amo et al., 2020b), and can be used as a positive control (**Fig. 1c**). All Cas9 transgenes are inserted into the *yellow* locus and are expressed by the same *vasa* germline promoter. Separately, we built two Copycat gene-drive constructs inserted into the *white* gene that produce two different gRNAs. Note that the two homology arms included as part of the CopyCat elements match each cut site of the gRNAs couple to ensure perfect homology and a proper HDR process. These transgenes were marked with a GFP marker instead to track its inheritance. Both Copycat lines share the *w2*-gRNA, which we validated in previous works (López Del Amo et al., 2020a, 2020b), and that was combined with the *w8*-gRNA or with the *w9*-gRNA (**Fig. 1d**). The PAM DNA sequences are crucial for target location recognition (Jinek et al., 2012), and these constructs present different PAM orientations depending on the gene-drive element used. The Copycat containing *w2,w8*-gRNAs display a PAM-out orientation as the two gRNAs PAMs' are facing opposite directions. In contrast, the *w2,w9*-gRNAs couple result in a PAM-in arrangement, where both PAMs are facing each other. All three gRNAs are located within a ~100 base pair DNA window, therefore, an approximate distance of 50 nucleotides separates paired-gRNA cut sites. (**Fig. 1d**).

Most importantly, the combination of either of the CopyCat lines with regular Cas9 produces similar blunt ends in both situations (**Fig. 1e**). However, the combination of both nickases with the two CopyCat transgenic lines result in four different scenarios: i) The nD10A generates 3' overhangs when combined with the Copycat containing the *w2,w9*-gRNAs (PAM-in) or ii) can also result in 5' overhangs when combined with the *w2,w8*-gRNAs couple (PAM-out). Instead, iii) the nH840A source combined with *w2,w9*-gRNAs (PAM-in) triggers 5'

overhangs or iv) 3' overhangs if combined with the *w2,w8*-gRNAs (PAM-out) CopyCat transgenic line (**Fig. 1e**). Altogether, our experimental architecture allows us to evaluate four different scenarios to test the feasibility of a nickase gene drive system.

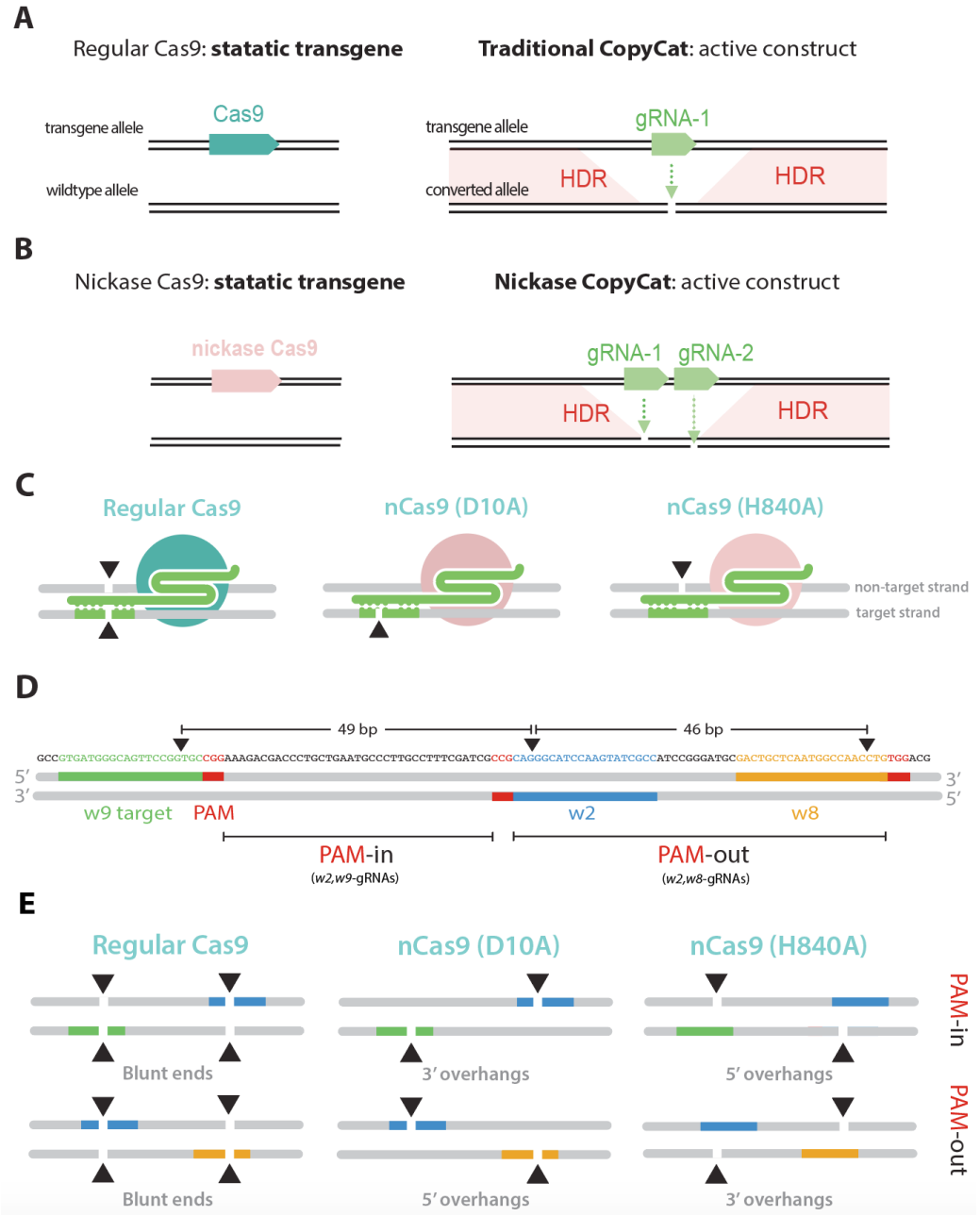

Fig.1. A nickase-based gene drive system promotes different overhang patterns. a. Schematic diagram of a traditional CopyCat gene-drive system. The gRNA cassette replaces the wildtype allele (converted allele) by DNA double-strand break and subsequent homology directed-repair (HDR) when combined with a Cas9 source. **b.** A static nickase Cas9 source is combined with a nickase Copycat containing two gRNAs targeting each complementary strand of the wildtype allele to spread the couple-gRNA cassette by HDR. **c.** The nD10A only cuts the target strand where the gRNA is bound. Instead, the nH840 cuts the non-target strand. **d.** Sequence and design of the paired-gRNAs in both PAM-out and PAM-in orientation. Paired-gRNAs are located ~50nt apart. Note that depicted gRNAs will be binding to the opposite strand when produced by complementarity. Red label indicates the PAM sequences (not included in the gRNA) that are crucial for DNA recognition. The black triangles mark the different cut sites associated with each gRNA **e.** The regular Cas9 introduces blunt ends when combined with either of the CopyCat elements. The nD10A and nH840, combined with paired-gRNAs binding to specific DNA strands, can generate 5' or 3' overhangs as they target different strands (target and non-target strand, respectively).

Both Cas9 nickases promote super-Mendelian inheritance of the CopyCat elements

To evaluate the efficiency of our gene-drive CopyCat elements, we used the same cross scheme in all cases. First, male flies containing either of the Cas9 sources (regular Cas9, nD10A or nH840A), were combined with the CopyCat lines to obtain F1 trans-heterozygous animals carrying both transgenes. Then, these F1 females were crossed to a white mutant line to evaluate biased inheritance in their F2 progeny. If the Copycat is not active, we should observe 50% inheritance of the GFP marker, which is integrated within the engineered cassette as mentioned above. Differently, if the CopyCat construct is able to promote HDR in the germline, it should display super-Mendelian inheritance (>50%) of the GFP-marked transgene. All the Cas9 sources, which carry the DsRed marker, should instead be inherited at ~50% inheritance (**Fig. 2a**).

We first combined the regular Cas9 with both CopyCat elements; in this experiment, we introduce two close-by DNA double-strand breaks producing the so-called multiplexing approach (**Fig.1e**), which already demonstrated its efficiency at biasing Mendelian inheritance (Champer et al., 2018). Here, both PAM-out and PAM-in CopyCat elements displayed similar super-Mendelian inheritance levels of ~97% (**Fig. 2b**). We did not observe significant differences between CopyCat elements when combined with the regular Cas9, suggesting that both gRNA-pairs would have similar efficiencies (*p-value*= 0.6721**,** see statistics **Supplementary Data 1**). In a previous work, we individually validated the *w2*-gRNA in a similar CopyCat arrangement that showed 90% super-Mendelian inheritance (López Del Amo et al., 2020a). Therefore, the addition of a second gRNA (w8 or w9) seems to somewhat boost the allelic conversion efficiency from 90% to ~97% in both cases. These results are in line with previous reports describing the use of an additional gRNA to increase gene drive performance (Champer et al., 2018).

After confirming the activity of the two gene-drive elements built to test the nickase gene drive, we turned our efforts towards evaluating the ability of a nickase-Cas9 to promote super-Mendelian inheritance in either of the four scenarios described previously (**Fig. 1e**). First, we crossed our nD10A transgenic line with both CopyCat strains carrying the tandem-gRNAs, and following the same experimental cross scheme (**Fig. 2a**). In this case, the nD10A nickase version displayed 93% super-Mendelian inheritance levels when combined with the CC(*w2,w8*) generating 5' overhangs. In contrast, the CopyCat element carrying the *w2,w9*-gRNAs (PAM-in), and generating 3' overhangs, was inherited in a Mendelian fashion (~50%) (**Fig. 2c; Supplementary Data 2**).

Next, we performed the experiment using the nH840A line and following the same cross scheme strategy (**Fig. 2a**). Here, the nH840A produced super-Mendelian inheritance rates of ~85% on average when combined with the CC(*w2,w9*) (PAM-in) that generated 5' overhangs. However, we observed 50% inheritance rates when the CC(*w2,w8*) (PAM-out) was combined with the nH840A that generated 3' overhangs (**Fig. 2c; Supplementary Data 2**). Importantly, we observed super-Mendelian inheritance using both nickase versions (D10A and H840A). It is important to note that the nD10A produced bias inheritance only when combined with the CopyCat element containing the *w2,w8*-gRNAs pair; instead, the nH840A triggered super-Mendelian inheritance when it was crossed to the CopyCat carrying the *w2,w9*-gRNAs couple. These two combinations, where gene-drive activity

was detected, have in common that they generated 5' overhangs. This observation indicates that gene-drive activity is only possible when particular overhangs are generated; and these results correlate with previous *in vitro* works showing that paired nicks only stimulated significant HDR levels when generating 5' overhangs using the nD10A (Mali et al., 2013; Ran et al., 2013).

Overall, the nD10A performed significantly better than the nH840A in terms of inheritance bias (*p-value* <0.0001, see statistics **Supplementary Data 2**), and this could be due to different cleavage rates between nickase versions. The *white* gene targeted for conversion in our system presents a tight linkage with the *yellow* gene where our nickase Cas9 sources are inserted, allowing us to evaluate the cutting rates looking at the F2 progeny. In fact, the nD10A version displayed 95% cutting efficiency, which is higher compared to the H840A that showed 91% cutting rates (*p-value*=0.0683; see statistics **Supplementary Data 1**). Altogether, these results represent the first example of a gene-drive system driven by a nickase Cas9 version, which introduces simultaneous nicks on both complementary strands to induce efficient allelic conversion mediated by HDR *in vivo*. Further, these results indicate that nickase gene-drive super-Mendelian inheritance can be only achieved through 5' overhangs generation.

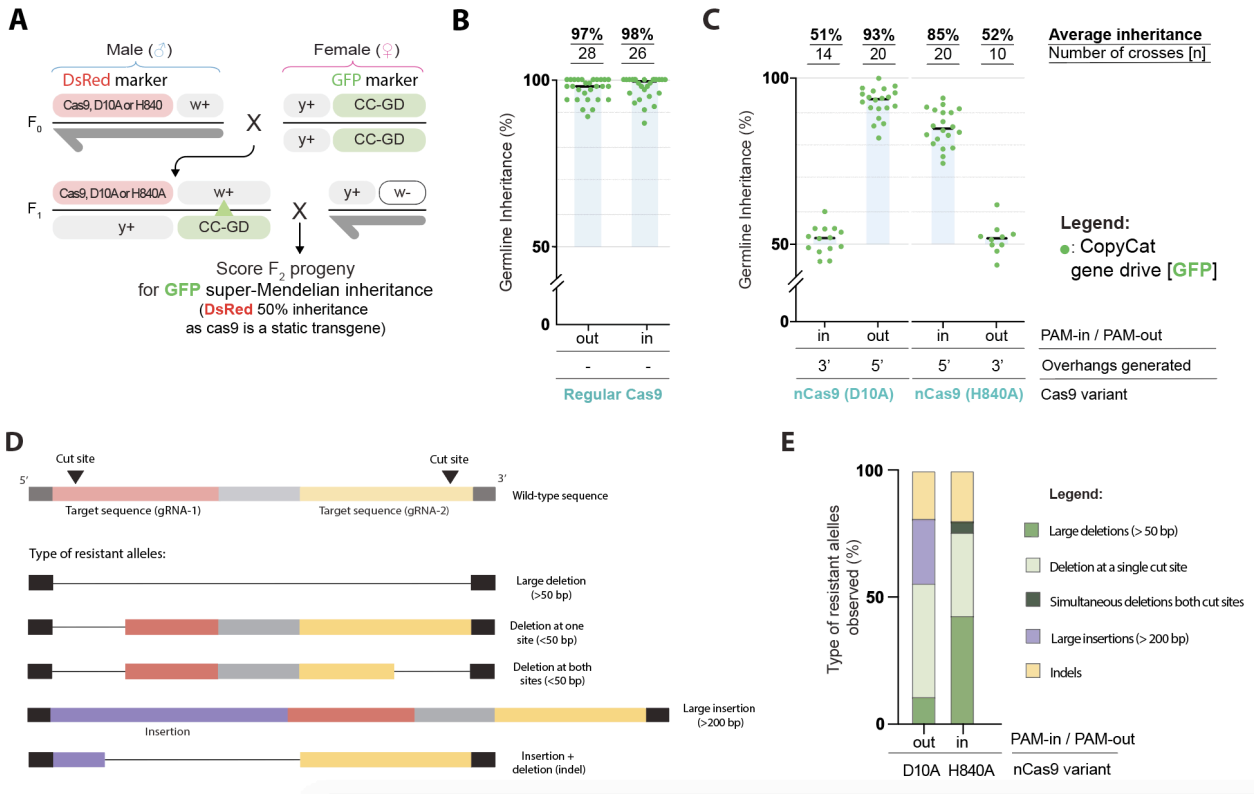

Fig.2. Super-Mendelian inheritance rates produced by nickase Cas9 versions when 5' overhangs are generated. a. All Cas9 sources (regular Cas9, nD10A and nH840A) and the CopyCat elements are inserted in the X chromosome (*yellow [y] and white [w]* genes, respectively). F0 males containing the regular Cas9 of either of the nickase versions were crossed to females containing either of the Copycat gene drives (CC-GD). F1 females carrying both transgenes were crossed to wildtype males to assess germline allelic conversion (green triangle indicates potential wildtype allele replacement) by scoring the GFP marker in the F2. **b.** Similar biased inheritance rates were observed when the regular Cas9 was combined with both CopyCat elements. **c.** The nD10A and the nH840A triggered super-Mendelian inheritance rates only when generating 5' overhangs. **d.** Schematic of observed resistant allele outcomes in the nickase-based gene-drive experiments. **e.** The nD10A (n=20) produced a high frequency of large insertions while the nH840A (n=24) produced bigger deletions between nick sites.

As we briefly mentioned above, when the allelic conversion mediated by the HDR process is not accurate, DNA double-strand breaks introduced by gene drives can produce resistant alleles at the target site. While resistant alleles generated by the regular Cas9 have been extensively characterized by multiple groups, including us (Champer et al., 2018; Gantz and Bier, 2015; Hammond et al., 2017; López Del Amo et al., 2020b), the types of resistant alleles generated by paired-nicks remain uncharacterized in a gene drive context. For this reason, we decided to evaluate and compare the type of resistant alleles generated by our nickase gene drive systems. Since the CopyCat's target is the *white* gene located in the X chromosome, and males have only one X chromosome, F2 males presenting *white* eye phenotype and GFP negative indicate *white* gene disruption and unsuccessful allelic conversion. These phenotypes allowed us to identify individuals carrying resistant alleles. Thus, we collected non-converted F2 males from either nickase-conditions that displayed gene drive activity, nD10A PAM-out, and nH840 PAM-in (**Fig. 2c**). We then performed DNA extraction from these animals and characterized them by Sanger sequencing. Among the sequences analyzed we observed five different classes of mutations for both PAM-out and PAM-in conditions: i) large deletions spanning both cut sites (>50 bp) ii) deletions (<50bp) occurring at only cut site while keeping the other cut site intact, iii) simultaneous deletions (<50bp) happening at both target sites but maintaining part of the sequence between cut sites , iv) large insertions (>200bp) and v) small insertions combined with small deletions appearing in the same individuals at the same cut site (indels) (**Fig. 2d; Supplementary Fig.1**).

First, we detected that the nH840A combined with PAM-in gRNAs displayed 42% of the total sequenced flies with large deletions ranging from 50 to 90 nucleotides (**Fig. 2e; Supplementary Fig. 1a**). This represents a significantly higher frequency of large deletions spanning both nick sites compared to the PAM-out condition that displayed only 5% (**Fig. 2e;** *p-value*= 0.0389, see statistics **Supplementary Data 3**).

Additionally, we observed large insertions (>200bp) when nD10A was combined with paired-gRNAs in a PAM-out orientation (**Supplementary Fig.1d**). In particular, 25% (5 out of 20) of the sequenced flies within this condition presented large insertions, being significantly higher than the nH840A combined with PAM-in gRNAs where we did not detect any large insertion event (**Fig. 2e**; *p-value*= 0.0143, see statistics **Supplementary Data 3**). Interestingly, the large insertions produced by the PAM-out gRNAs represented partial HDR occurrences containing portions of the engineered gene-drive allele. We detected either part of the U6 promoter right after the left homology arm or the synthetic 3xP3 promoter with an incomplete piece of the GFP marker located after the right homology arm of the gene drive element (**Supplementary Fig. 1d**). This outcome is consistent with previous observations when a multiplexing gene drive, using regular Cas9 and gRNAs in a PAM-out orientation, induced the formation of insertions resulting from partial HDR events (Champer et al., 2018).

The rest of the categories described above, and including single cuts at only one target site, simultaneous mutations at both cut sites or indels, did not show significant differences between the nickase genotypes (**Fig. 2e**; see statistics **Supplementary Data 3**). Further, we also sequenced the resistant alleles generated by the regular Cas9, and confirmed that the gRNAs employed in this work are active, as we found mutations at all target sites within the genotypes that produced super-Mendelian inheritance with the regular Cas9 and both nickase

versions (**Supplementary Fig.1**). Overall, our Sanger sequencing analysis showed different repair outcomes when using distinct nickase versions, and this could inform future nickase-based gene drive strategies.

DISCUSSION

In this work, we describe a gene-drive system based on nickase versions of Cas9 that promotes super-Mendelian inheritance in *Drosophila*. We first show that both nD10A and nH840A can produce efficient HDR in the germline, but only when the two nicks in the DNA generate 5' overhangs. Our sequence characterization of events that fail to convert the wildtype allele to gene drive, indicates that the nH840A combined with PAM-in gRNAs produced higher rates of large deletions compared to the nD10A PAM-out arrangement. Also, while the PAM-out condition triggered the formation of large insertions, we did not observe any large insertion when analyzing resistance alleles produced by the nH840A, suggesting that different modes of DNA repair may be triggered when specific nickases are used.

In our experiments, the nD10A produced higher super-Mendelian rates than the nH840A. As mentioned above, this could be due to differences in cleavage activities between both nickase versions. In fact, it has also been shown in cell culture that the nH840A presents less cleavage activity as it produced lower indel rates when disrupting the *EMX-S1* gene (Gopalappa et al., 2018). Also, we could not discard that distinct time-windows cleavage between gRNAs couples, which need to cut simultaneously, may impact on HDR efficiencies since both nickase versions showed super-Mendelian inheritance with different paired-gRNAs. While previous studies did not detect meaningful HDR rates when using the nH840A (Bothmer et al., 2017; Mali et al., 2013; Ran et al., 2013), we were able to show for the first time efficient HDR rates achieved by gRNAs in a PAM-in configuration when 5' overhangs were generated using the nH840A. This observation indicates that the nH840A could be a viable option under specific conditions for future nickase-based designs.

Although the main scope of this work was to obtain a proof-of-concept for a Cas9-nickase gene drive, we observed higher super-Mendelian rates when using the regular Cas9. We believe that a nickase gene-drive requires the coordinated action of both gRNAs cutting at the same time to induce efficient HDR. Instead, when the regular Cas9 is used, a single cut from either of the paired-gRNAs can induce HDR as they produce double-stranded DNA breaks. Furthermore, while any failure of the first gRNA would result in a small indel, the second gRNA would still be able to cut and trigger a second round of potential conversion, which would also explain why our control displayed a slightly higher inheritance rate when compared to the nickases. For this reason, it is important that future nickase gene-drive would thoroughly test the gRNA-pair to maximize coordinated action in time.

Regarding the resistant alleles' formation, we provide evidence that our nH840A transgene combined with paired-gRNAs in a PAM-in configuration frequently generated large deletions between the spaced nicks; a scenario that we did not detect when using gRNAs in a PAM-out with the nD10A. This property could be harnessed to boost gene-drive efficiency when targeting essential genes or critical protein domains. In this strategy, the gene-drive element, carrying a DNA rescue or recoded sequence, replaces the wildtype allele while

restoring gene functionality of these vital genes to ensure animal viability and gene drive spread. Most importantly, if resistant alleles occur due to unsuccessful allelic conversion, these mutations should be detrimental producing non-viable animals. However, small mutations occurring at essential genes can still produce a few viable escapees. Therefore, large deletions induced by a gene-drive system using the nH840A in a PAM-in configuration, should help ensure the removal of individual escapees carrying small indels that survived within a population (Terradas et al., 2021).

We also wondered if a nickase gene-drive arrangement could help reduce the formation of resistant alleles as DNA nicks are usually repaired efficiently. Yet, we also detected resistant alleles caused by single DNA nicks, which could be due to single non-repaired nicks converted to double-strand breaks and then fixed by NHEJ (Kuzminov, 2001). We recognize this could be a limitation of the system as mutations produced at a single target site by DNA nicks would be an obstacle for further gene drive propagation. Single nicks are poor HDR inducers (Vriend et al., 2016), therefore, having one mutation at only one target site would be enough to avoid gene drive spread. However, our proof-of-concept nickase gene-drive method is amenable to further optimization, and future studies will focus on improving its efficiency. For example, our proof-of-principle design only tested the efficiency of a nickase gene-drive system inducing DNA paired-nicks that are ~50 nucleotides apart, yet, our strategy could be adapted to generate distinct offset distances and evaluate the effect on HDR efficiency. In fact, efficient HDR has been observed with offset distances ranging from 20 to 100 base pairs (Vriend et al., 2016).

Future nickase-gene drive approaches could also explore other potential advantages such as increasing specificity and reducing off-target effects. As two independent cleavage events need to happen coordinately to obtain the desired modification, paired nicks improved specificity while reducing off-target effects when disrupting the *EMX1* gene using human cell culture (Ran et al., 2013). The potential off-target events accumulation while a gene-drive propagates through a population is a concern and an important aspect to consider. Recently, off-target effects caused by gene drives were predicted using validated algorithms and posterior in vivo-targeted deep sequencing using *Anopheles* mosquitoes (Garrood et al., 2021). In this study, off-targets were almost undetectable if using promoters restricting Cas9 expression to the germline under non-overlapping laboratory cage studies. It is important to note though that this still needs to be tested in wild populations where the Cas9 will be present for longer periods compared to cage-based laboratory experiments. Indeed, a nickase gene-drive system could be tested in *Anopheles*, or other species such as *Aedes* or *Culex* mosquitoes that present a genome three times bigger than *Anopheles (*Main et al., 2021; Severson et al., 2004*)*, and where off-target effects may be more pervasive due to genome size. Furthermore, gene drives also demonstrated their ability to bias Mendelian inheritance using mice (Grunwald et al., 2019; Weitzel et al.), and a nickase-based gene-drive system should be portable to these animals to explore potential benefits to reduce off-target effects observed when editing mammalian embryos (Aryal et al., 2018). Altogether, our proof-of-principle study represents the first step towards the development of next-generation nickase-based gene-drive designs bringing potential advantages to future applications of these technologies. We hope that our work will spur the use of nickase-based gene-drive systems for improved population control while encouraging its implementation in a broader range of organisms.

ACKNOWLEDGMENTS

The research reported in this manuscript was supported by the University of California, San Diego, Department of Biological Sciences, by the Office of the Director of the National Institutes of Health under award number DP5OD023098 (to V.M.G), and by the National Institute of Allergy and Infectious Diseases under the award number R01AI162911 (to V.M.G). V.L.D.A and V.M.G are authors on a patent filed by the University of California, San Diego (Provisional Application Serial No. 63/254,753) that is related to the nickase gene-drive system described in this work.

AUTHOR CONTRIBUTIONS

V.L.D.A and V.M.G conceived the project. V.L.D.A designed and obtained the nickase gene-drive constructs in *Drosophila*. V.L.D.A and S.S.J performed the experiments. V.L.D.A, V.M.G and S.S.J performed the figure visualizations. V.L.D.A wrote the manuscript, which was edited by all the authors.

DECLARATION OF INTERESTS

V.M.G. has equity interests in Synbal, Inc. and Agragene, Inc., companies that may potentially benefit from the research results and also serves on both companies' Scientific Advisory Board and on the Board of Directors of Synbal, Inc. The terms of this arrangement have been reviewed and approved by the University of California, San Diego in accordance with its conflict-of-interest policies. V.L.D.A, and S.S.J declare no competing interests.

MATERIAL AND METHODS

Fly rearing and crosses

All flies were kept on standard food with a 12/12-hour day/night cycle. Fly stocks are kept at 18°C, and all experimental crosses were performed at 25°C. All flies were anesthetized during our experiments using CO_2. F_0 crosses from gene-drive experiments were made in pools of 3-6 virgin females crossed to 3-6 males. F_1 experiments were always made in single pairs to track editing events happening singularly in the germline. The F_2 progeny was scored as male or female and sorted for a fluorescent marker (DsRed and/or GFP) using a Leica M165 F2 Stereomicroscope with fluorescence as an indicator of transgene inheritance rates. All experiments were performed in a high-security ACL2 (Arthropod Containment Level 2) facility built for gene drive purposes in the Division of Biological Sciences at the University of California, San Diego. Crosses were made in polypropylene vials (Genesee Scientific Cat. #32-120), and all flies were frozen for 48 hours before being removed from the facility, autoclaved, and discarded as biohazardous waste.

Plasmid construction

DNA constructs were built using NEBuilder HiFi DNA Assembly Master Mix (New England BioLabs Cat. #E2621) and transformed into NEB 10-beta electrocompetent *E.coli* (New England BioLabs Cat. #3020). DNA was extracted using a Qiagen Plasmid Midi Kit (Qiagen Cat. #12143) and sequenced by Sanger sequencing at Genewiz. Primers used for cloning can be found in the Key Resources Table below. Final sequences of all constructs will be available at NCBI ahead of publication.

Transgenic line generation and genotyping

We outsourced embryo injections to Rainbow Transgenic Flies, Inc. All DNA constructs were injected into our lab's isogenized Oregon-R (Or-R) strain to ensure consistent genetic background throughout experiments. Plasmid templates were co-injected with a Cas9-expressing plasmid (pBSHsp70-Cas9 was a gift from Melissa Harrison & Kate O'Connor-Giles & Jill Wildonger [Addgene plasmid #46294; http://n2t.net/addgene:46294; RRID: Addgene_46294]). We received the injected generation 0 (G_0) animals, then we intercrossed the hatched adults in small pools (3-5 males x 3-5 females), and screened the G_1 flies for a fluorescent marker (DsRed for Cas9 versions and GFP for gene-drive elements, both fluorescences in the eye), which was indicative of transgene insertion. Lastly, we established homozygous lines from single transformants by crossing to Or-R. As the Cas9 transgene is inserted into the *yellow* gene disrupting it, homozygous flies for the Cas9 versions can be identified once flies display a yellow body color. Similarly for the Copycat constructs that are integrated into the *white* gene, homozygous flies for the CopyCat elements display a white eye phenotype. Stocks were sequenced by PCR and Sanger sequencing to confirm proper transgene insertion.

DNA extraction from single flies

To sequence resistant alleles, we extracted genomic DNA from individual males following the method described by Gloor GB and colleagues (Gloor et al., 1993). In brief, we used 50ul of the extraction buffer to squish single flies in a PCR tube. Next, we placed them into the PCR machine (Proflex PCR system, *Applied Biosystems*) for 1 hour at 37℃ followed by 5 minutes at 95℃ to inactivate the proteinase K. Then, we added to each DNA sample 200uL of water to obtain a total of 250uL per sample. Lastly, we used 1-5uL in a 25uL PCR reaction covering the gRNA cut sites in the *white* gene for Sanger sequencing analysis.

Sanger sequencing of individuals carrying resistance alleles

We amplified a DNA region covering the gRNA cut sites using the v1564 and v1565 oligos (see oligos list below). The obtained amplicon was then sequenced by Sanger sequencing to determine the quality of the resistant alleles using the v478 oligo. When we obtained lower-quality traces, we performed a second Sanger sequencing reaction from the other side of the amplicon to confirm the quality of the mutation with either the v659 or v1571 primers. Primers used for resistance allele sequencing can be found in the Key Resources Table.

Microscopy

Adult flies were anesthetized using CO2 to select individuals for crossing experiments. Their phenotypes were analyzed using a Leica M165 FC Stereo microscope to properly prepare the experimental crosses. Inheritance analysis of the transgenes marked with fluorescence was evaluated using the same microscope. DsRed marker implies presence of the Cas9 cassettes while GFP fluorescence indicates presence of the CopyCat transgenes.

Statistical analysis

We used GraphPad Prism 9 and Adobe Illustrator to generate all the graphs. Statistical analyses were performed using GraphPad Prism 9. In **Fig. 2b**, we applied an unpaired *t test* to compare inheritance rates when using the regular Cas9 (**Supplementary Table 1**). Additionally, One-Way Anova and Tukey's multiple comparison test to evaluate differences between super-Mendelian rates in our nickase gene-drive experiments in **Fig. 2c** (**Supplementary Table 2**). For evaluating the differences in proportions for deletions and insertion events in **Fig. 2d**, we used Fisher's exact test (**Supplementary Table 3**).

RESOURCES TABLE

Supplementary Table 1 - List of primers used in this study

Oligos for resistant allele sequencing analysis	
Name	**Primer**
v478	GCTGGTCAACCGGACACGCGG
v659	AGGGAGCCGATAAAGAGGTCATCC
v1571	GGCTCATCGCAGATCAGAAG
v1564	TTATGGACGAACGCCGTGAAATTG
v1565	GCCGGATTGTAGTTGGTAGGAC
Oligos for molecular cloning	
Nickase cas9 constructs:	
v1146	CTGTCTCAGCTGGGAGGCGACAAAAGGCCGGC
v1144	GAATTAGATCCACCGGTTTGACGTCTCCGTGGGCATCGG
v1145	TGCCCACGGAGACGTCAAACCGGTGGATCTAATTCAATTAGAGACTAATTCAATTAGAGC
v0725	CCGATGCTGTACTTCTTGTCGGCTGCTGGGACTCCGTGGATAC
CopyCat gene-drive constructs:	
v0724	GACAAGAAGTACAGCATCGGCCTG
v0377	GTCGCCTCCCAGCTGAGACAG
611	CTGCGGCGATCGAAAGGCAAGGGCATTCAGC
v0992	CCCGGGCGAGCTCGCCTAGGCTGTGGACGCCAAGGAGATG
615	GCCTTTCGATCGCCGCAGACGTCATTTTCAACGTCCTCGATAGTATAGTGGTTAGTATCC
v0689	GCACCGACTCGGTGCCAC
v1015	GTGGCACCGAGTCGGTGCTTTTTTGCTCACCTGTGATTGCTCCTAC
v0973	CCTAGGCGAGCTCGCCCGGGGATCTAATTCAATTAGAGACTAATTCAATTAGAGC
v1016	GAGGACGTTGAAAATGACGTCCGGAACTGCCCATCACGGCCAAAAGTTCG
612	GGCATCCAAGTATCGCCATCCGGGATGCGACTG
1067	ACGTCATTTTCAACGTCCTCGATAGTATAGTGGTTAG

v1017	GATGGCGATACTTGGATGCCCCTAtGCGAGCTCGCCCGGGGATC

SUPPLEMENTARY TABLES TABLES

Data S1.xlsx, Related to Figure 2. Phenotypical scoring of the two CopyCat gene-drives elements combined with regular cas9.

Data S2.xlsx, Related to Figure 2. Phenotypical scoring of the two CopyCat gene drives combined with either nickase Cas9 version.

Data S3.xlsx, Related to Figure 2 and Supplementary Figure 1. Comparison of deletion and insertion events between both nickase versions for resistant allele formation.

REFERENCES

Adolfi, A., Gantz, V.M., Jasinskiene, N., Lee, H.-F., Hwang, K., Terradas, G., Bulger, E.A., Ramaiah, A., Bennett, J.B., Emerson, J.J., et al. (2020). Efficient population modification gene-drive rescue system in the malaria mosquito Anopheles stephensi. Nat. Commun. *11*, 5553.

Aryal, N.K., Wasylishen, A.R., and Lozano, G. (2018). CRISPR/Cas9 can mediate high-efficiency off-target mutations in mice in vivo. Cell Death Dis. *9*, 1099.

Bier, E. (2021). Gene drives gaining speed. Nat. Rev. Genet.

Bothmer, A., Phadke, T., Barrera, L.A., Margulies, C.M., Lee, C.S., Buquicchio, F., Moss, S., Abdulkerim, H.S., Selleck, W., Jayaram, H., et al. (2017). Characterization of the interplay between DNA repair and CRISPR/Cas9-induced DNA lesions at an endogenous locus. Nat. Commun. *8*, 13905.

Caldecott, K.W. (2008). Single-strand break repair and genetic disease. Nat. Rev. Genet. *9*, 619–631.

Chafin, D.R., Vitolo, J.M., Henricksen, L.A., Bambara, R.A., and Hayes, J.J. (2000). Human DNA ligase I efficiently seals nicks in nucleosomes. EMBO J. *19*, 5492–5501.

Champer, J., Liu, J., Oh, S.Y., Reeves, R., Luthra, A., Oakes, N., Clark, A.G., and Messer, P.W. (2018). Reducing resistance allele formation in CRISPR gene drive. Proc. Natl. Acad. Sci. U. S. A. *115*, 5522–5527.

Champer, J., Chung, J., Lee, Y.L., Liu, C., Yang, E., Wen, Z., Clark, A.G., and Messer, P.W. (2019). Molecular safeguarding of CRISPR gene drive experiments. Elife *8*.

Gantz, V.M., and Bier, E. (2015). Genome editing. The mutagenic chain reaction: a method for converting heterozygous to homozygous mutations. Science *348*, 442–444.

Gantz, V.M., and Bier, E. (2016). The dawn of active genetics. Bioessays *38*, 50–63.

Gantz, V.M., Jasinskiene, N., Tatarenkova, O., Fazekas, A., Macias, V.M., Bier, E., and James, A.A. (2015). Highly efficient Cas9-mediated gene drive for population modification of the malaria vector mosquito Anopheles stephensi. Proc. Natl. Acad. Sci. U. S. A. *112*, E6736–E6743.

Garrood, W.T., Kranjc, N., Petri, K., Kim, D.Y., Guo, J.A., Hammond, A.M., Morianou, I., Pattanayak, V., Joung, J.K., Crisanti, A., et al. (2021). Analysis of off-target effects in CRISPR-based gene drives in the human malaria mosquito. Proc. Natl. Acad. Sci. U. S. A. *118*.

Gloor, G.B., Preston, C.R., Johnson-Schlitz, D.M., Nassif, N.A., Phillis, R.W., Benz, W.K., Robertson, H.M., and Engels, W.R. (1993). Type I repressors of P element mobility. Genetics *135*, 81–95.

Gopalappa, R., Suresh, B., Ramakrishna, S., and Kim, H.H. (2018). Paired D10A Cas9 nickases are sometimes more efficient than individual nucleases for gene disruption. Nucleic Acids Res. *46*, e71.

Grunwald, H.A., Gantz, V.M., Poplawski, G., Xu, X.-R.S., Bier, E., and Cooper, K.L. (2019). Super-Mendelian inheritance mediated by CRISPR-Cas9 in the female mouse germline. Nature *566*, 105–109.

Hammond, A., Galizi, R., Kyrou, K., Simoni, A., Siniscalchi, C., Katsanos, D., Gribble, M., Baker, D., Marois, E., Russell, S., et al. (2016). A CRISPR-Cas9 gene drive system targeting female reproduction in the malaria mosquito vector Anopheles gambiae. Nat. Biotechnol. *34*, 78–83.

Hammond, A.M., Kyrou, K., Bruttini, M., North, A., Galizi, R., Karlsson, X., Kranjc, N., Carpi, F.M., D'Aurizio, R., Crisanti, A., et al. (2017). The creation and selection of mutations resistant to a gene drive over multiple generations in the malaria mosquito. PLoS Genet. *13*, e1007039.

Hyodo, T., Rahman, M.L., Karnan, S., Ito, T., Toyoda, A., Ota, A., Wahiduzzaman, M., Tsuzuki, S., Okada, Y., Hosokawa, Y., et al. (2020). Tandem Paired Nicking Promotes Precise Genome Editing with Scarce Interference by p53. Cell Rep. *30*, 1195–1207.e7.

Jinek, M., Chylinski, K., Fonfara, I., Hauer, M., Doudna, J.A., and Charpentier, E. (2012). A programmable dual-RNA-guided DNA endonuclease in adaptive bacterial immunity. Science *337*, 816–821.

Kuzminov, A. (2001). Single-strand interruptions in replicating chromosomes cause double-strand breaks. Proc. Natl. Acad. Sci. U. S. A. *98*, 8241–8246.

Kyrou, K., Hammond, A.M., Galizi, R., Kranjc, N., Burt, A., Beaghton, A.K., Nolan, T., and Crisanti, A. (2018). A CRISPR-Cas9 gene drive targeting doublesex causes complete population suppression in caged Anopheles gambiae mosquitoes. Nat. Biotechnol. *36*, 1062–1066.

Li, M., Yang, T., Kandul, N.P., Bui, M., Gamez, S., Raban, R., Bennett, J., Sánchez C, H.M., Lanzaro, G.C., Schmidt, H., et al. (2020). Development of a confinable gene drive system in the human disease vector. Elife *9*.

López Del Amo, V., Leger, B.S., Cox, K.J., Gill, S., Bishop, A.L., Scanlon, G.D., Walker, J.A., Gantz, V.M., and Choudhary, A. (2020a). Small-Molecule Control of Super-Mendelian Inheritance in Gene Drives. Cell Rep. *31*, 107841.

López Del Amo, V., Bishop, A.L., Sánchez C, H.M., Bennett, J.B., Feng, X., Marshall, J.M., Bier, E., and Gantz, V.M. (2020b). A transcomplementing gene drive provides a flexible platform for laboratory investigation and potential field deployment. Nat. Commun. *11*, 352.

Main, B.J., Marcantonio, M., Johnston, J.S., Rasgon, J.L., Brown, C.T., and Barker, C.M. (2021). Whole-genome assembly of Culex tarsalis. G3 *11*.

Mali, P., Aach, J., Stranges, P.B., Esvelt, K.M., Moosburner, M., Kosuri, S., Yang, L., and Church, G.M. (2013). CAS9 transcriptional activators for target specificity screening and paired nickases for cooperative genome engineering. Nat. Biotechnol. *31*, 833–838.

Port, F., Chen, H.-M., Lee, T., and Bullock, S.L. (2014). Optimized CRISPR/Cas tools for efficient germline and somatic genome engineering in Drosophila. Proc. Natl. Acad. Sci. U. S. A. *111*, E2967–E2976.

Ran, F.A., Hsu, P.D., Lin, C.-Y., Gootenberg, J.S., Konermann, S., Trevino, A.E., Scott, D.A., Inoue, A., Matoba, S., Zhang, Y., et al. (2013). Double nicking by RNA-guided CRISPR Cas9 for enhanced genome editing specificity. Cell *154*, 1380–1389.

Reyes, G.X., Kolodziejczak, A., Devakumar, L.J.P.S., Kubota, T., Kolodner, R.D., Putnam, C.D., and Hombauer, H. (2021). Ligation of newly replicated DNA controls the timing of DNA mismatch repair. Curr. Biol. *31*, 1268–1276.e6.

Severson, D.W., DeBruyn, B., Lovin, D.D., Brown, S.E., Knudson, D.L., and Morlais, I. (2004). Comparative genome analysis of the yellow fever mosquito Aedes aegypti with Drosophila melanogaster and the malaria vector mosquito Anopheles gambiae. J. Hered. *95*, 103–113.

Simoni, A., Hammond, A.M., Beaghton, A.K., Galizi, R., Taxiarchi, C., Kyrou, K., Meacci, D., Gribble, M., Morselli, G., Burt, A., et al. (2020). A male-biased sex-distorter gene drive for the human malaria vector Anopheles gambiae. Nat. Biotechnol. *38*, 1054–1060.

Terradas, G., Buchman, A.B., Bennett, J.B., Shriner, I., Marshall, J.M., Akbari, O.S., and Bier, E. (2021). Inherently confinable split-drive systems in Drosophila. Nat. Commun. *12*, 1480.

Vriend, L.E.M., and Krawczyk, P.M. (2017). Nick-initiated homologous recombination: Protecting the genome, one strand at a time. DNA Repair *50*, 1–13.

Vriend, L.E.M., Prakash, R., Chen, C.-C., Vanoli, F., Cavallo, F., Zhang, Y., Jasin, M., and Krawczyk, P.M. (2016). Distinct genetic control of homologous recombination repair of Cas9-induced double-strand breaks, nicks and paired nicks. Nucleic Acids Res. *44*, 5204–5217.

Wang, H., and Hays, J.B. (2007). Human DNA mismatch repair: coupling of mismatch recognition to strand-specific excision. Nucleic Acids Res. *35*, 6727–6739.

Wang, Q., Liu, J., Janssen, J.M., Le Bouteiller, M., Frock, R.L., and Gonçalves, M.A.F.V. (2021). Precise and broad scope genome editing based on high-specificity Cas9 nickases. Nucleic Acids Res. *49*, 1173–1198.

Wang, Y., Zhao, J., Duan, N., Liu, W., Zhang, Y., Zhou, M., Hu, Z., Feng, M., Liu, X., Wu, L., et al. (2018). Paired CRISPR/Cas9 Nickases Mediate Efficient Site-Specific Integration of F9 into rDNA Locus of Mouse ESCs. International Journal of Molecular Sciences *19*, 3035.

Weitzel, A.J., Grunwald, H.A., Levina, R., Gantz, V.M., Hedrick, S.M., Bier, E., and Cooper, K.L. Meiotic Cas9 expression mediates genotype conversion in the male and female mouse germline.

Xu, X.-R.S., Gantz, V.M., Siomava, N., and Bier, E. (2017). CRISPR/Cas9 and active genetics-based trans-species replacement of the endogenous -L2 CRM reveals unexpected complexity. Elife *6*.

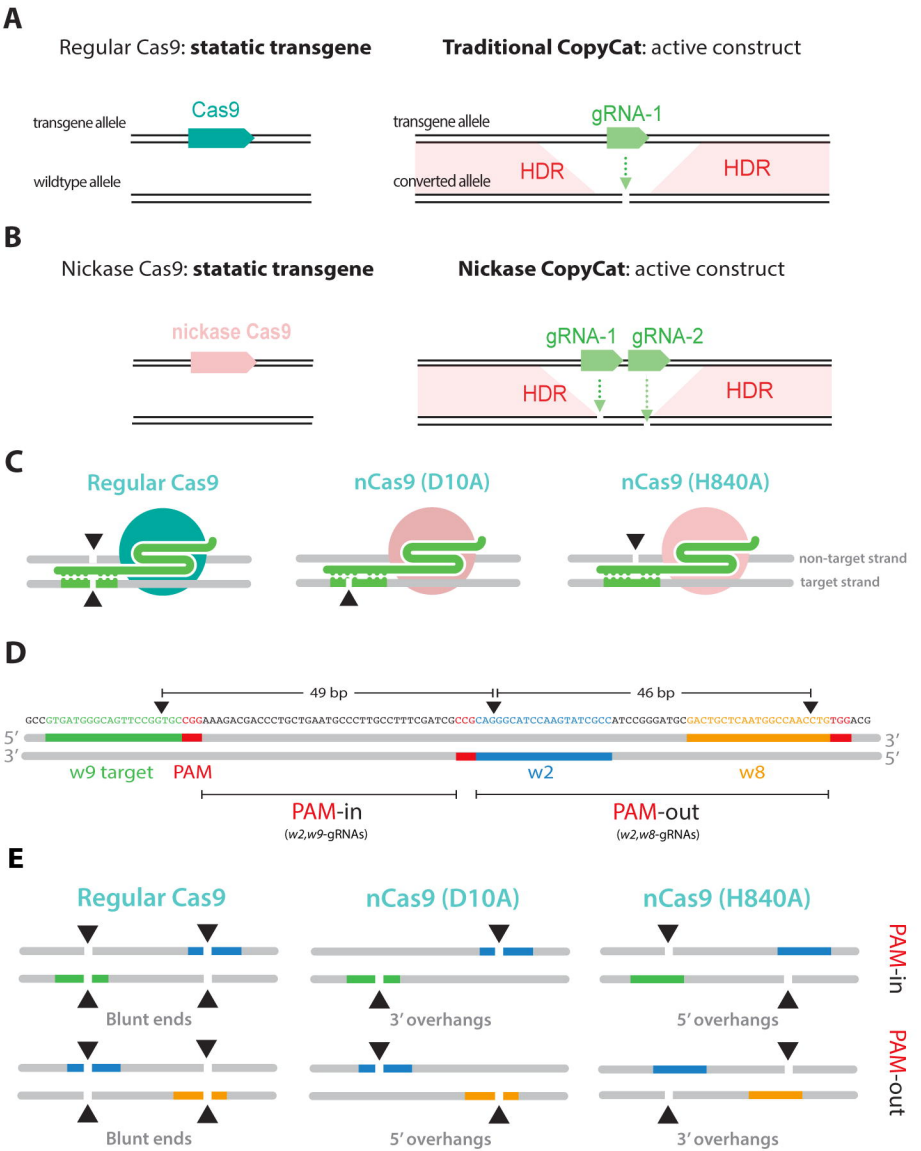
A
Regular Cas9: statatic transgene
Traditional CopyCat: active construct
transgene allele
Cas9
wildtype allele
transgene allele
gRNA-1
converted allele
HDR
HDR
B
Nickase Cas9: statatic transgene
Nickase CopyCat: active construct
nickase Cas9
gRNA-1
gRNA-2
HDR
HDR
C
Regular Cas9
nCas9 (D10A)
nCas9 (H840A)
non-target strand
target strand
D
49 bp
46 bp
GCCGTGATGGGCAGTTCCGGTGCCGGAAAGACGACCCTGCTGAATGCCCTTGCCTTTCGATCGCCGCAGGGCATCCAAGTATCGCCATCCGGGATGCGACTGCTCAATGGCCAACCTCTGGACG
5′
3′
3′
5′
w9 target
PAM
w2
w8
PAM-in
(w2,w9-gRNAs)
PAM-out
(w2,w8-gRNAs)
E
Regular Cas9
nCas9 (D10A)
nCas9 (H840A)
Blunt ends
3′ overhangs
5′ overhangs
Blunt ends
5′ overhangs
3′ overhangs
PAM-in
PAM-out

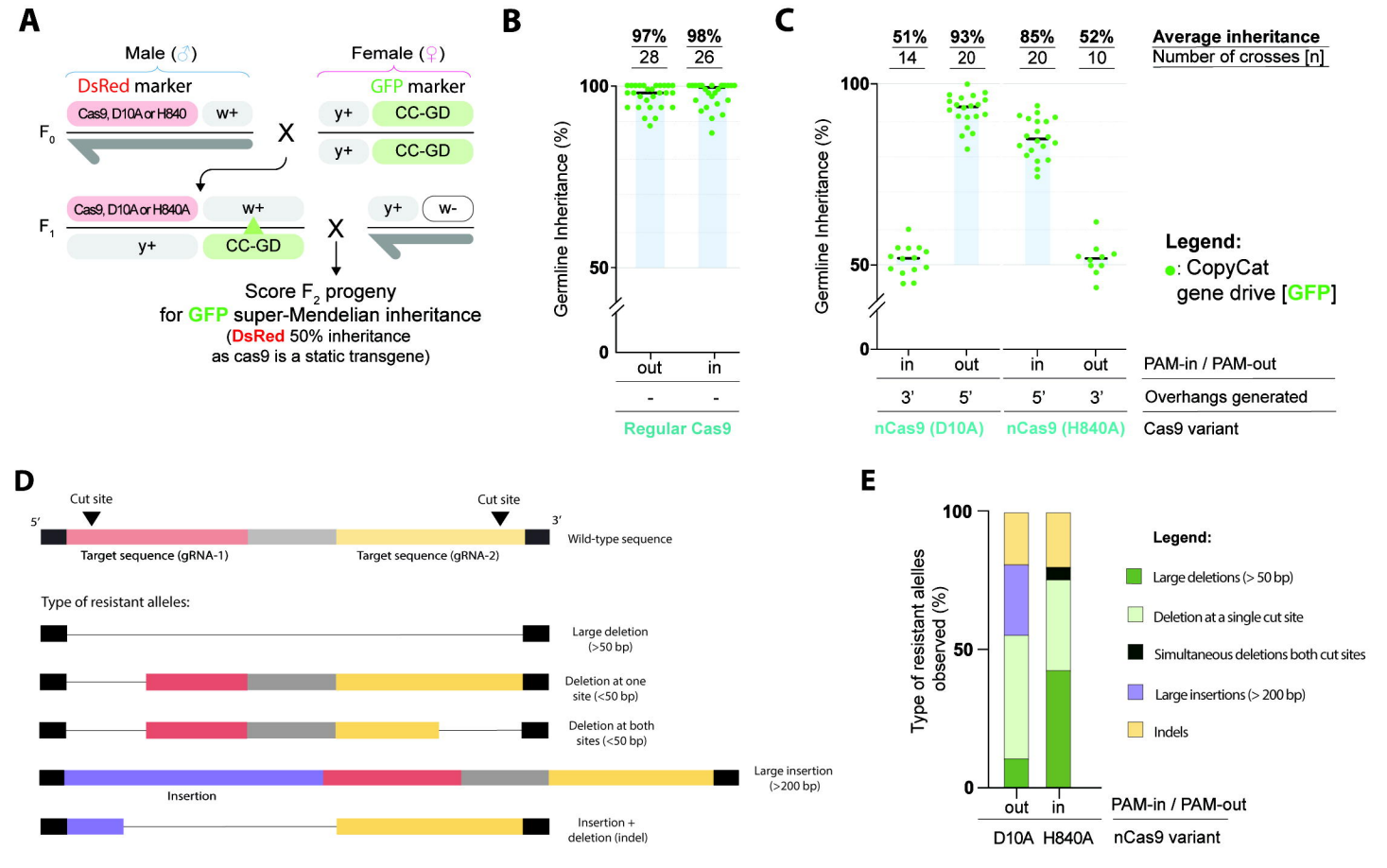
A
Male (♂)
Female (♀)
DsRed marker
GFP marker
Cas9, D10A or H840
w+
y+
CC-GD
F0
X
Cas9, D10A or H840A
w-
F1
Score F2 progeny
for GFP super-Mendelian inheritance
(DsRed 50% inheritance
as cas9 is a static transgene)
B
97%
98%
28
26
Germline Inheritance (%)
100
50
0
out
in
Regular Cas9
C
51%
93%
85%
52%
14
20
20
10
Average inheritance
Number of crosses [n]
Legend:
: CopyCat
gene drive [GFP]
PAM-in / PAM-out
Overhangs generated
Cas9 variant
nCas9 (D10A)
nCas9 (H840A)
D
Cut site
5′
3′
Target sequence (gRNA-1)
Target sequence (gRNA-2)
Wild-type sequence
Type of resistant alleles:
Large deletion
(>50 bp)
Deletion at one
site (<50 bp)
Deletion at both
sites (<50 bp)
Insertion
Large insertion
(>200 bp)
Insertion +
deletion (indel)
E
Type of resistant alleles
observed (%)
Legend:
Large deletions (> 50 bp)
Deletion at a single cut site
Simultaneous deletions both cut sites
Large insertions (> 200 bp)
Indels
PAM-in / PAM-out
nCas9 variant
D10A
H840A